J Mater Sci (2007) 42:9736–9745
DOI 10.1007/s10853-007-1978-y

Reaction of 316L stainless steel with a galvanizing bath

Ke Zhang · Nai-Yong Tang · Frank E. Goodwin · Scott Sexton

Received: 15 February 2007 / Accepted: 2 July 2007 / Published online: 20 August 2007

Abstract Type 316L stainless steel (316L SS), commonly used as pot roll material, was tested in an industrial Zn–Al galvanizing bath, with an effective Al content of 0.2 wt.%. Samples welded to the supporting roll arms and sides of the sink roll experienced heavy dross buildup. Samples placed at locations away from the incoming strip generally experienced much less dross buildup. Dross particles within the buildup on samples attached to supporting roll arms were small in size but numerous while particles on samples welded to the sides of the sink roll were much larger. SEM-EDS analyses indicated that the buildup consisted of two layers. The inner layer was the product of the corrosive reaction of 316L SS with the bath metal, and the outer layer was formed by dross particles built up on the inner reaction layer. The intermetallic phase, which formed at the reaction front of the samples was the inhibition compound Fe_2Al_5 containing some Mo and Cr. The formation of this intermetallic layer provided a thermodynamically favourable base for the attachment and further buildup of suspended dross particles on the sample surfaces.

K. Zhang (✉) · N.-Y. Tang
Teck Cominco Metals Ltd, Product Technology Centre, 2380, Speakman Drive, Mississauga, ON, Canada L5K 1B4
e-mail: keith.zhang@teckcominco.com

N.-Y. Tang
e-mail: naiyong.tang@teckcominco.com

F. E. Goodwin
International Lead Zinc Research Organization, Inc, 2525 Meridian Parkway, Suite 100, Durham, NC 27713, USA
e-mail: fgoodwin@ilzro.org

S. Sexton
Nucor Steel – Crawfordsville Division, 4537 S. Nucor Road, Crawfordsville, IN 47933, USA
e-mail: ssexton@ns-ind.com

Introduction

On a continuous galvanizing line (CGL), pot hardware, including rolls and supporting bearings, is used to guide incoming steel strips through the Zn–Al bath and, therefore, is subjected to an arduous environment of elevated temperatures and a corrosive media, the molten Zn–Al alloy. Galvanizers are being challenged increasingly to improve the performance of pot hardware in order to achieve better product quality and operation efficiency. Pot hardware made of metallic materials is known to react with galvanizing baths to form intermetallic phases [1–5]. Brunnock et al. [4] carried out extensive tests of coated and uncoated stainless steels, as well as low carbon steel, in a molten Zn–Al alloy (Al content of 0.135 wt.% and Fe content of 0.03%) at two temperatures 455 and 480 °C. They found that all uncoated stainless steels were aggressively attacked by this alloy. Austenitic stainless steel generally outperformed martensitic stainless steel, which, in turn, performed better than low carbon steel. In fact 316L stainless steel (316L SS) has been widely used in the galvanizing industry to construct pot equipment owing to its good combination of resistance to molten Zn–Al galvanizing alloy attack, compatible mechanical properties and reasonable cost. With the recent revitalized interest in galvanizing pot hardware, significant attention is being paid to the steel with particular emphasis on dross formation and buildup on the steel in various zinc baths [6, 7].

When immersed in Zn–Al baths, 316L SS reacts with the molten metal to form a reaction layer. The reaction and the resultant intermetallic phases vary with the global test parameters such as bath chemistry (notably the Al content) and temperature. The reaction and its product are also influenced by the local environment, such as the flow pattern and its proximity to the incoming strip. Laboratory

studies at the Product Technology Centre of Teck Cominco Metals Ltd. uncovered some common characteristics of the interaction between the 316L SS and galvanizing baths. The reaction always initiated with the formation of an Al-rich layer ($Fe_2Al_5Zn_x$ type) [8]. The reaction front then advanced further into the test materials, leaving behind a Zn-rich zone. The thickness of the reaction layer increased noticeably with the test time at an early stage and then reached a quasi-steady state, where there was little change in the thickness of the reaction layer with test time. The change in thickness of the reaction layer was also accompanied by a complicated evolution of the phase constituents of the reaction layer, which directly influences dross buildup on pot hardware. However, questions remain on whether 316L SS behaves differently in a continuous galvanizing pot where rolls are constantly rotating and the molten metal is constantly flowing. In other words, the environment is much more dynamic in nature in a production bath. An on-line dynamic test carried out recently revealed that there was a significant difference in dross buildup on 316L SS samples placed at different locations in the galvanizing pot [9]. It became apparent that a systematic on-line investigation was warranted to unravel the performance of 316L SS in the galvanizing pot.

In this study, on-line testing of 316L SS was carried out in a galvanizing line. To better understand the reaction of 316L SS with the galvanizing bath and the mechanisms of dross buildup on the steel, both static and dynamic tests were concurrently conducted. The objectives of the study were to uncover the reaction mechanisms and to examine the morphology and size of the buildup pertinent to sample locations as well as test conditions. In this paper, selected results are presented along with a discussion of the corrosion mechanism of 316L SS in a continuous galvanizing bath.

Experimental

Test setup

Test pieces of 316L SS in the form of blocks and rods were commercially procured. The chemical compositions of a rod sample are provided in Table 1. Five-rod samples, 25.4 mm in diameter and 152.4 mm in length, were hooked to a specially designed sample holder. The holder was welded to the rear left side of the galvanizing pot away from the ingot charging area. A dynamic test sample assembly consisted of a rod and two blocks. The rods were 12.7 mm in diameter and 76.2 mm in length, and the blocks were 25.4 mm cubes with a 12.7 mm diameter hole drilled on one face. The rod was inserted into the holes of two opposite blocks, which were tap-welded to a pre-determined location on the pot hardware. Such an arrangement enabled two different sample geometries to be evaluated. In total, 38 assemblies were welded to stabilizer roll arms, sink roll arms and sink roll edges, sides and necks as depicted in Fig. 1.

Table 1 Chemical analysis results for a 316L SS rod used in the on-line test

Materials	Chemical composition (mass %)								
	C	Mn	P	S	Si	Ni	Cr	Mo	Co
316L SS	0.026	1.22	0.037	0.028	0.51	10.04	16.15	2.05	0.13

Experimental procedure

The galvanizing line operates at a pot temperature of around 460 °C. The targeted effective Al content of the bath was 0.2 wt.%. A bath Al measurement system was installed to continuously monitor and record the bath temperature and effective Al content for the entire duration of the testing. During the test period, the bath temperature was maintained at about 460 ± 4 °C. The effective Al content of the bath, however, fluctuated between 0.17 wt.% and 0.22 wt.%. For the static test, the samples were dipped for 1, 4, 24, 168 and 336 h. The dynamic test lasted for the entire galvanizing campaign of 504 h.

After the on-line testing, cross-sections through the as-tested samples were prepared following a standard sample preparation procedure. Dross buildup on the samples was first examined with a light optical microscope. The microstructural details of the buildup were further studied using a Jeol JSM-5800LV Scanning Electron Microscope (SEM) equipped with an Energy Dispersive Spectrometer (EDS).

The essence of this investigation is to study the reaction of the 316L SS with the Zn–Al bath and its effect on the dross build-up. Thus, the depths of reaction layers on samples were measured instead of the weight or thickness loss. By simply measuring the changes in sample weight or dimensions, the severity of the reaction of the steel with the Zn–Al bath could be misinterpreted because results of such a measurement depend strongly how the reaction products, consisting of the residual Zn overlay, the buildup layer and the reaction layer are removed. Image analysis software Image-Pro Plus 4.0 was used to measure the thickness of the reaction layers, which was based on a point-to-point measurement (see Fig. 2a and e). Efforts were made to distinguish the reaction layer with the outside buildup layer and to exclude the attached top dross particles. The data reported represent the average of at least 20 measurements on four different micrographs.

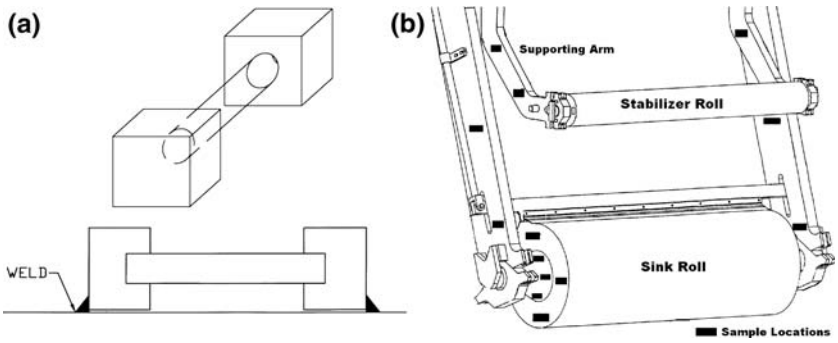

Fig. 1 Schematics of (**a**) dynamic test sample assembly and (**b**) locations of samples welded to the pot hardware

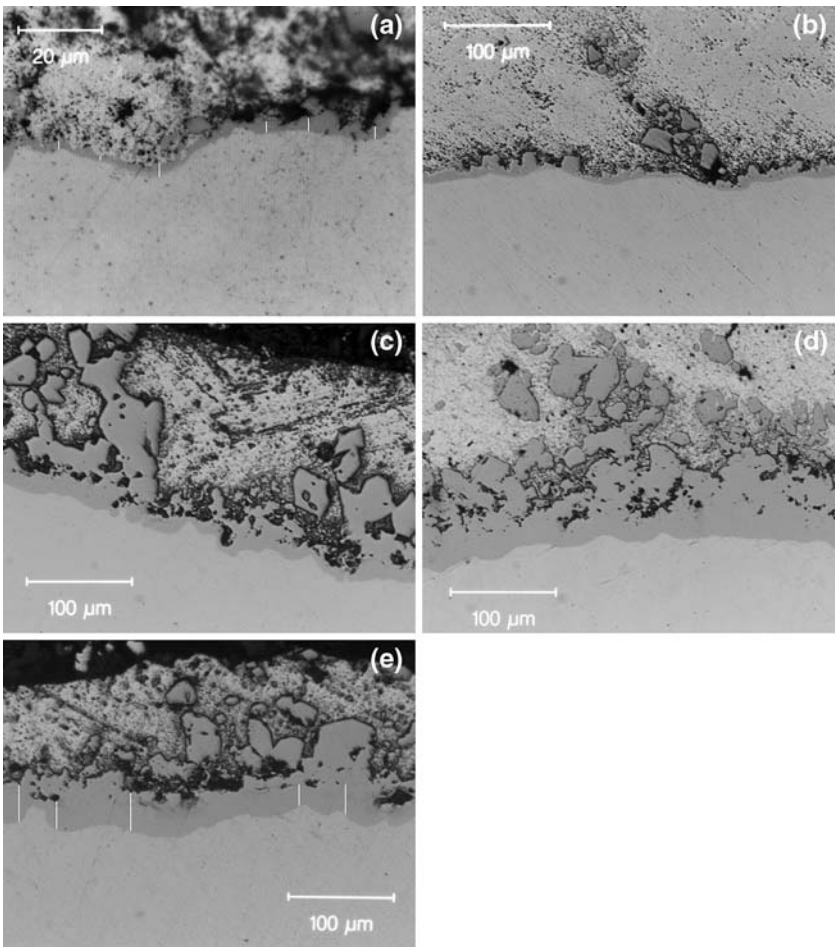

Fig. 2 Light optical micrographs of cross-sections of 316L SS samples statically dipped in the galvanizing pot for various lengths of time: (**a**) 1 h; (**b**) 4 h; (c) 24 h; (**d**) 168 h and (**e**) 336 h

Results

Static testing

Figure 2a through e show optical microscopic images of as-polished cross-sections of 316L SS samples subjected to the static test for various lengths of time. A continuous reaction layer was visible after 1 h of testing. The thickness of the reaction layer increased with increased testing time for up to 168 h with a gradual buildup of dross particles outside the layers. Thereafter, the effect of the test duration on the thickness of the reaction layer was not obvious (Table 2). The results are comparable to the findings in our earlier laboratory static dipping tests of 316L SS in a

Table 2 Thickness of the reaction layer as a function of test duration in hours

Test material	Thickness of the reaction layer (µm)				
	1	4	24	168	336
316L SS	1.1	3.4	10.9	30.1	33.4

Zn–0.23 wt.%Al bath [8]. Two types of particles appear to be involved in the dross buildup on the reaction layer. One type has an intimate connection with the reaction layer and appears to be part of the reaction product, while the other type is loosely attached and originated from suspended dross particles in the galvanizing bath. The amount of loose particles appears to increase with the dipping time.

The buildup, particularly in the vicinity of the reaction layer, was studied in detail using SEM-EDS techniques. Figure 3 shows cross-sections of samples submerged in the galvanizing bath for 4, 24, 168 and 336 h. For the sample tested for 4 h, the reaction of the 316L SS with the galvanizing bath resulted in a reaction layer of non-uniform thickness, thin in some locations and thicker in other locations. The thinner layer was dark in appearance. EDS analyses of the thin dark layer revealed that it was based on $Fe_2Al_5Zn_x$ containing on average about 50.2% Al, 28.8% Fe, 19.3% Zn, 1.1% Mo and 0.6% Cr (atomic percentages unless noted otherwise). The hue of a thick reaction layer frequently covered a wide grey scale with the reaction front appearing quite dark but fading away towards the end zone. The dark front was similar in composition to the thinner dark layer described above; however, the lighter area contained much more Zn. Its typical composition was 51.8% Zn, 30.0% Al, 16.8% Fe, 1.2% Mo and 0.2% Cr. Within the lighter area, there were some darker particles (arrows) containing 53.1% Al, 30.5% Fe, 15.1% Zn, 0.9% Mo, and 0.4% Cr ($Fe_2Al_5Zn_x$ phase). The evolution and transformation of the reaction layer were much more evident on samples suspended in the bath for an extended period of time as can be seen in Fig. 3b–d. As the dipping time increased, more and more darker areas emerged within the reaction layer and changed into particle-like shapes as shown in Fig. 4. The compositions of those areas were similar to those of top dross particles ($Fe_2Al_5Zn_x$) but with a small amount of Mo, averaging 54.3% Al, 29.6% Fe, 15.2% Zn, and 0.9% Mo. Some of these particles grew outward to the bath and connected with top dross particles loosely attached to the reaction layer. The attached top dross particles averaged 55.17% Al, 31.96% Fe, and 12.87% Zn.

Dynamic testing

The main objective of the dynamic test was to investigate the effect of local environment on dross buildup on 316L SS. This was achieved by attaching sample assemblies of rods and blocks to different locations on all types of submerged bath hardware. Figure 5 shows optical microscopic views of as-polished cross-sections of block samples welded to the arms of the sink roll and the stabilizer roll. In general, only small amounts of particles were directly attached to the reaction layer on the sample surface while the majority of the particles were simply entrapped in the residual Zn coatings on the samples when the hardware was withdrawn from the pot upon completion of the test. The sizes of the particles were less than 100 μm. In comparison to the statically dipped samples shown in Figs. 2 and 3, there were significantly more dross particles present in the Zn overlay in the dynamically tested samples. It can also be seen that the amount of dross particles entrapped in the Zn overlays was quite different for samples welded on different types of arms and on different locations of an arm.

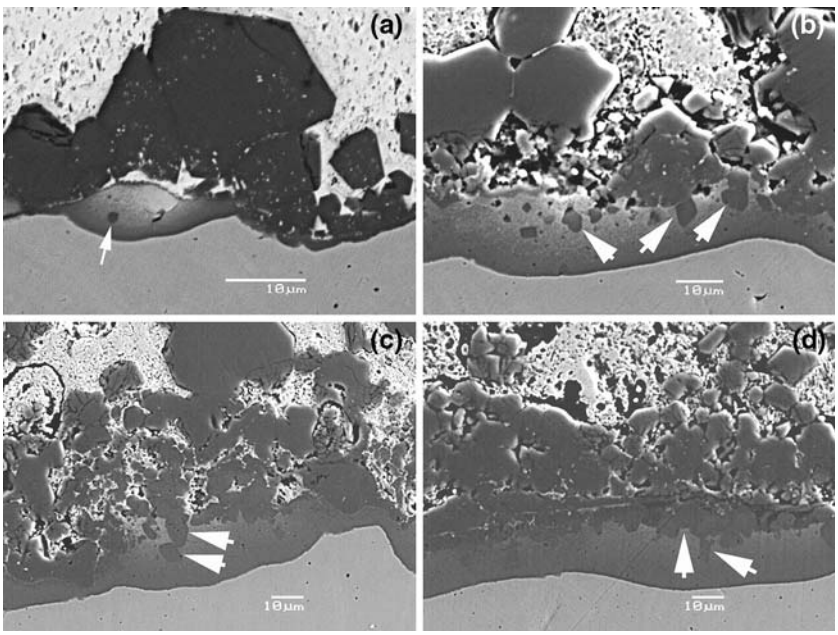

Fig. 3 SEM micrographs of buildup on the 316L SS samples: (**a**) 4 h; (**b**) 24 h; (**c**) 168 h; and (**d**) 336 h

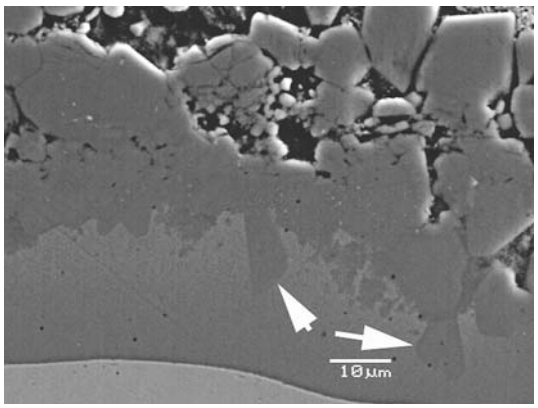

Fig. 4 Formation of particle-like areas within the reaction layer

Similar situations were observed for the rod-type samples as depicted in Fig. 6. Sample assemblies welded to the arms are "static" in nature. The differences in the buildup on these two groups of samples described above stemmed mainly from the differences in sample location, and probably also in the sample shape and withdrawal speed.

Dross buildup on samples welded to the sink roll was noticeably different. As can be seen in Figs. 7 and 8, big dross particles with a size of up to 500 μm were present and were intimately attached to the sample surface via the reaction layer. These big particles had the appearance of mono-crystallite. A few dross particles existed in the thin Zn overlay above the big particles. For samples welded to the neck of the sink roll (Fig. 8b), a cluster of dross particles was attached to the surface of the rod sample while big particles built up on the block sample (Fig. 8a). This observation has shed some light on the origin of the big particles.

Close examination of the buildup at high magnification using SEM-EDS techniques indicated clearly that the reaction layer evolved and transformed during the test. The reaction layer consisted of bands of different contrast and black pockets (Fig. 9). The reaction front typically displayed a dark contrast and contained about 53.7% Al, 29.8% Fe, 14.5% Zn, 1.3% Mo, and 0.7% Cr. The band with a lighter contrast contained more Zn but less Al and Fe with an average composition of 45.7% Al, 25.1% Fe, 27.8% Zn, 1.2% Mo and 0.2% Cr. Similar to the statically tested samples, the black pockets were particle-like in shape with an average composition of 54.6% Al, 30.5% Fe, 13.5% Zn, 1.2% Mo and 0.3% Cr. Some particles within the reaction layer connected with big top dross particles, which normally contained 55.4% Al, 32.5% Fe and 12.2% Zn. Other than small amounts of Mo and Cr, the particles formed within the reaction layer were chemically the same as the outside top dross particles. This once again revealed the transformation of 316L SS into top dross particles with an extended exposure to the galvanizing bath.

For samples welded to the sides of the sink roll, some "foreign" particles were also detected in the overlay and were identified as Stellite 6 and 316L SS particles by EDS analyses. Figure 10 shows those particles that were entrapped in the overlay above the big dross particles in the buildup. The former is believed to be wear debris from the pot roll bearings and the latter could either originate from the pot roll as a result of strip rubbing against its surface or from the flare-up when the sample assembly was tap-welded to the side of the sink roll. The circumferences of those "foreign" particles reacted with the bath to form an Al-rich layer. The reaction of those particles with the bath would

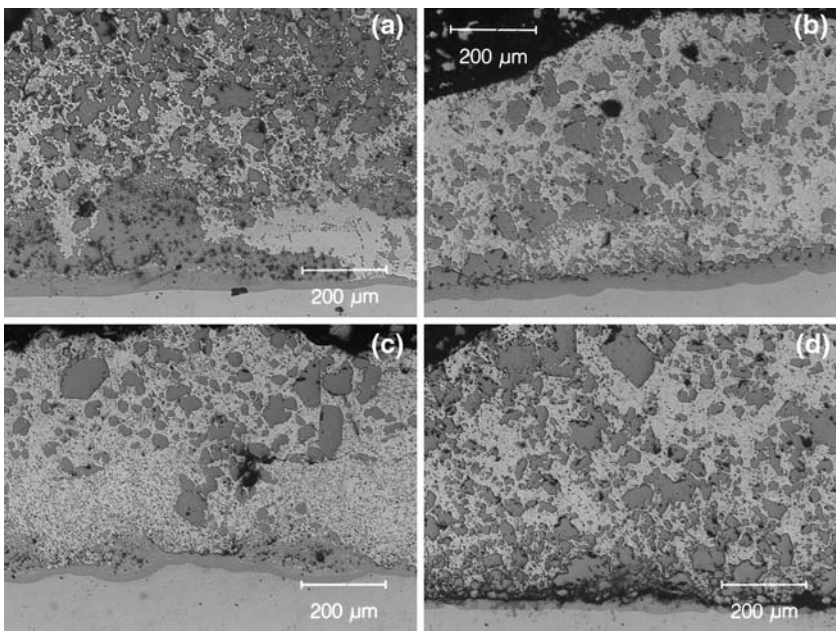

Fig. 5 Light optical micrographs of cross-sections of 316L SS block samples welded at: (**a**) a front stabilizer roll arm; (**b**) a rear stabilizer roll arm; (**c**) the bottom of a sink roll arm; and (**d**) the top of a sink roll arm

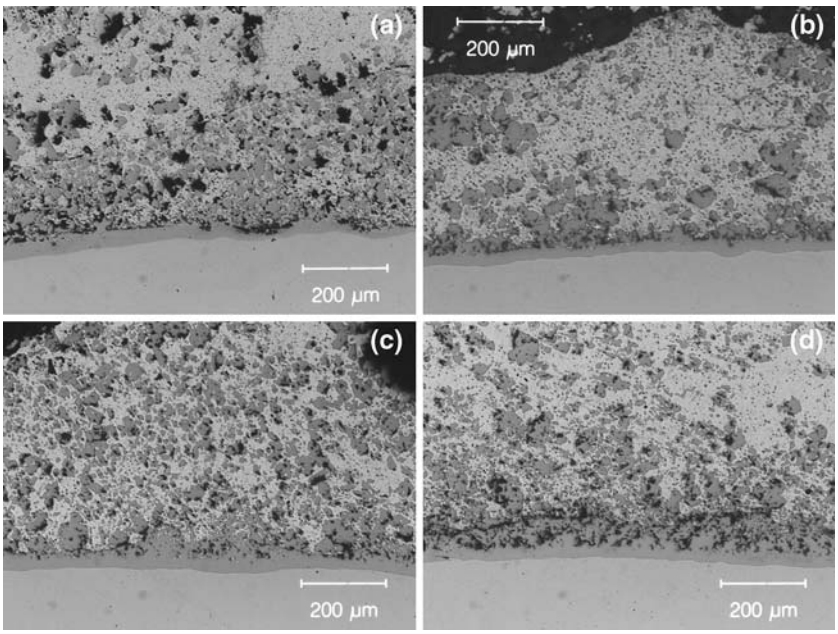

Fig. 6 Light optical micrographs of cross-sections of 316L SS rod samples welded at: (**a**) a front stabilizer roll arm; (**b**) a rear stabilizer roll arm; (**c**) the bottom of a sink roll arm; and (**d**) the top of a sink roll arm

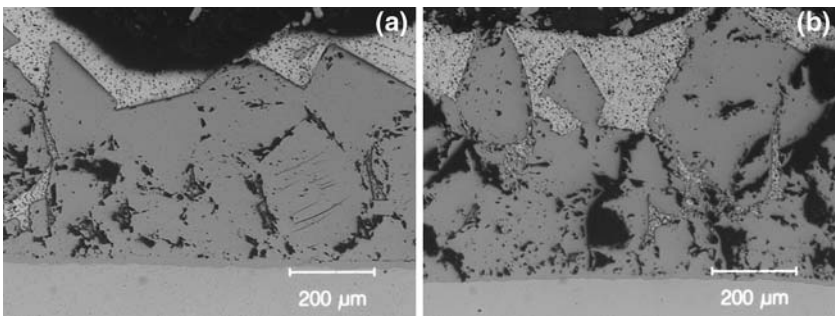

Fig. 7 Light optical micrographs of cross-sections of 316L SS samples welded at the sink roll edge: (**a**) block sample and (**b**) rod sample

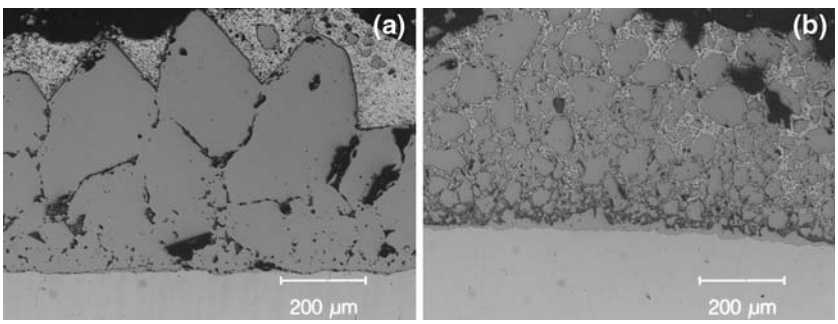

Fig. 8 Light optical micrographs of cross-sections of 316L SS samples welded at a sink roll neck: (**a**) block sample and (**b**) rod sample

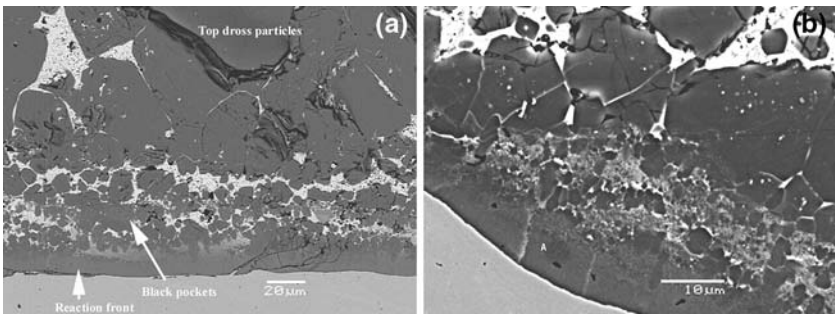

Fig. 9 SEM micrographs of the reaction interfaces for (**a**) a 316L SS block sample welded to the edge of a sink roll and (**b**) a 316L SS rod sample welded to the rear of a stabilizer roll arm

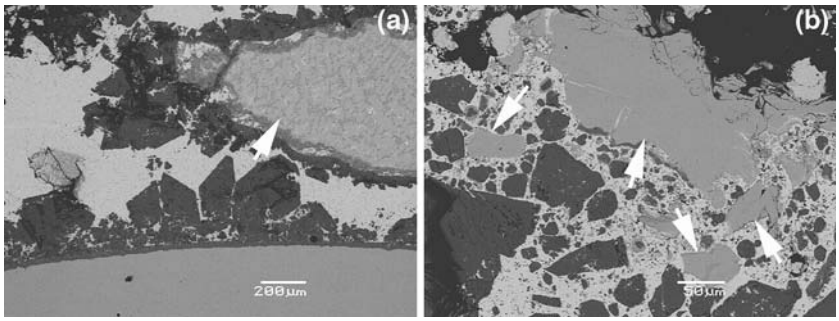

Fig. 10 SEM micrographs of a 316L SS rod sample welded to a side wall of a sink roll: (**a**) entrapped Stellite 6 debris and (**b**) entrapped 316L SS particles

transform them into top dross particles even for the Satellite 6 debris [10], contributing to the dross buildup.

Discussion

The results of this study indicate that 316L SS reacts similarly in an industrial galvanizing bath and in a laboratory Zn–Al bath with comparable compositions (effective Al of about 0.2 wt.%). Regardless of where the samples were placed, in a relatively stagnant location or in a more turbulent place, top dross particles were always built upon a compact and continuous reaction layer rather than directly on the steel surface. For samples statically tested in an industrial galvanizing pot, the dross buildup on the surface proceeded gradually with the development of the reaction layer. While the majority of top dross particles attached loosely to the reaction layer, small amounts of particles were intimately connected with the layer and some of them appeared to grow from the layer. As for the reaction layer, its thickness initially increased with increasing exposure time, and the reaction front ($Fe_2Al_5Zn_x$ type) moved into the depths of the test materials, leaving behind a Zn-rich zone. For samples welded to the pot hardware, large amounts of dross particles were built up on sample surfaces. Significant amounts of small dross particles were present on samples welded to the supporting arms (stationary) while much larger particles were attached to those welded to the sides of the sink roll (rotational).

The thicknesses of the reaction layers in the statically tested samples were experimentally measured in this study and are depicted in Fig. 11. Linear regression analyses of the results revealed clearly that a rate equation, $D = k\sqrt{t} + C$, described the experimental results very well, where D is the thickness of the reaction layer, t the dipping time, k the rate constant and C a constant. Therefore, the reactions were diffusion-controlled as would be expected from the fact that the reaction layers were continuous and compact. As a result, the reaction rates were determined by the diffusivity of the dominant reactant in the reaction layer. Eventually, the growth of the reaction layer became less obvious with further increases of the dipping time.

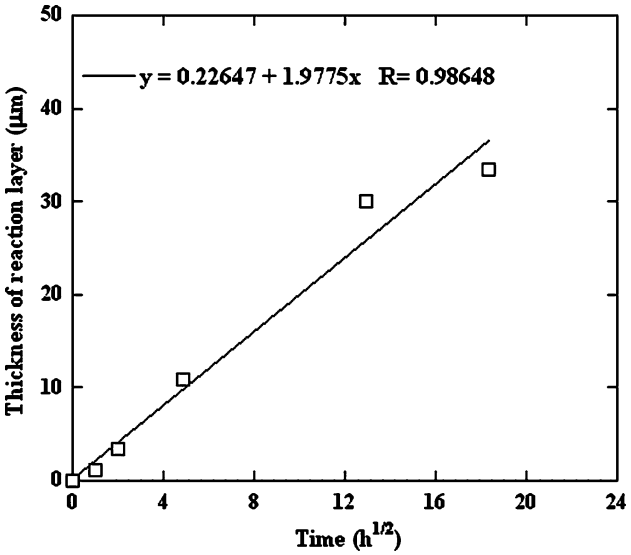

Fig. 11 The thicknesses of the reaction layers are linearly proportional to the square root of the dipping time

Results from on-line testing clearly indicate that dross buildup on 316L SS was the result of a reaction between the steel and the galvanizing bath as well as the interaction of this reaction layer with dross particles suspended in the galvanizing bath. The sharp difference between the buildup on samples welded to the arms and to the sink roll is particularly interesting. It appears that Fe dissolution from the incoming strip played a critical role in the buildup process. Generally, samples welded to the arms were farther away from the strip, and dross buildup on these samples was less severe than on those welded to the sides of the sink roll. Moreover, dross particles attached to samples welded to the sides of the sink roll were much larger in size. These observations suggest that dross particles were not homogeneously distributed within the galvanizing pot. There appear to be many more dross particles in the V region where the strip enters the bath, contacts the sink roll, and exits the pot. The quantity of dross particles and the volume of the bath in which they were found have not been predicted with currently available computational analysis [11]. Our observations have

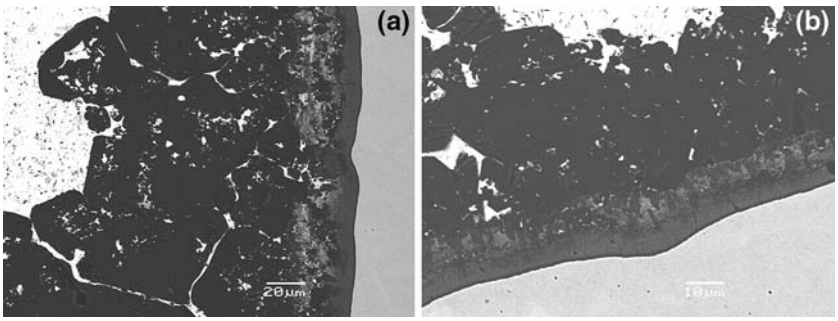

Fig. 12 Close-up views of the buildup of large dross particles on samples welded to the neck of the sink roll: (**a**) block sample and (**b**) rod sample

established that, in the transient period following the initial contact of the steel substrate and the molten galvanizing alloy, the local chemistry at the coating/substrate interface deviates significantly from the bulk bath chemistry. The local Fe concentration is estimated to be about one order of magnitude higher than the equilibrium Fe solubility. Fe atoms dissolved from the strip could not diffuse far enough away from the interface before the strip passed around the sink roll with the Fe-rich liquid being squeezed out from the coating/substrate interface. As a result, a large amount of dross particles formed in the vicinity of the sink roll. Some dross particles attached to samples placed in this region. The large particles built on samples welded to the sides of the sink roll look like mono-crystallites grown from a single nucleus. However, a careful examination of those particles revealed that they were the results of agglomeration of small dross particles as can be seen in Fig. 12. The morphology of the buildup on the rod samples welded to the neck of the sink roll shown in Fig. 8b provided convincing evidence that agglomeration was in progress. The rotation of the sink roll and the movement of the incoming strip could create a situation in which smaller dross particles have ample opportunity to collide with each other and agglomerate.

316L SS is a highly alloyed steel with the addition of significant amounts of Cr for enhanced corrosion and oxidation resistance. In the original design of the alloy, the addition of Ni to the steel was mainly to stabilize the austenitic structure for enhanced ductility and impact strength but also to help increase its resistance to corrosion by neutral chloride solution and other oxidizing acids. A small amount of Mo increases resistance to pitting attack by chloride solutions [12]. In galvanizing baths containing a relatively high Al level of 0.2%, 316L SS behaved rather differently in comparison to interstitial free (IF), low carbon, and low alloy steels. For IF steel, the reaction between the steel and the bath resulted in a $Fe_2Al_5Zn_x$ layer, dubbed the inhibition layer for its role in suppressing the reaction between Zn and Fe. However, the inhibition layer is believed to grow towards the bath [13], and the inhibition effect is frequently short-lived. The inhibition layer would not grow to more than a couple of micrometres thick before it broke down via "outbursts" after being immersed in the Zn–Al bath for a few minutes. On the contrary, the reaction layer formed on 316L SS, although $Fe_2Al_5Zn_x$ in nature, could grow quite thick. It is very stable although the incubation time for the formation of the reaction layer could be quite long, possibly due to the existence of a surface oxide skin. The cause of such a vastly different behaviour of the $Fe_2Al_5Zn_x$ compound is unknown. It could be that the compatibility of the compound with an austenitic substrate is much better than with a ferritic substrate. The growth of the reaction layer is most likely diffusion-controlled and follows a parabolic law. In the growth process, the reaction front moved towards the material, and complicated phase transformation occurred in the region behind the reaction front. Among the alloy elements, Cr and Ni appeared to have little effect on the stability of the reaction layer. They were quickly dissipated into the bath since they were thermodynamically more stable in the melt. On the other hand, Mo appears to play a role in stabilizing the reaction layer and has been detected within the reaction layer and even in the transformed areas.

Based on observations from the current on-line study, coupled with previous laboratory investigations on the reaction between 316L SS and Zn–Al baths, mechanisms of reaction and dross buildup on this type of steel can be contemplated as follows. When 316L SS was immersed in the galvanizing bath, the oxide layer formed on the surface initially prevented the direct contact of the steel with the molten metal (almost non-wetting). As a result, there was little change in the test sample when the immersion time was relatively short. Dross particles suspended in the bath were unable to attach to the 316L SS surface covered by the oxide skin. As shown in Fig. 3a, floating top dross particles in the bath did not attach to the surface of the sample being tested for 1 h. In fact, only a very limited area of the static testing bar had a Zn overlay forming on the surface when it was withdrawn from the galvanizing bath after 1 h of exposure. With further increases in dipping time, the oxide layer was dissipated, probably through reaction with the bath metal. A fresh steel surface was exposed, paving the way for the reaction between 316L SS and the bath. The reaction of 316L SS with the molten

Zn–Al alloy starts with the formation of an Fe_2Al_5 layer on the sample surface as seen in Fig. 3b. Top dross particles, also of Fe_2Al_5 type, start to attach to this layer to minimize the free energy of the system due to their chemical and structural similarity. Following the formation of dross buildup on the reaction layer, it appears that Al atoms diffused toward the reaction front are mostly captured and consumed by the dross particles covering up the reaction layer, leaving only a small portion available for the growth of the reaction layer. As a result, only Zn atoms are ample in supply. The evolution of the reaction layer observed in this study suggests that Al atoms in the previously formed reaction layer continue moving forward to push the reaction front inward while the vacant Al sites in the reaction layer are substitutionally occupied by Zn atoms. This is why the reaction front is always Al-rich and appears dark while the rest of the reaction layer becomes increasingly Zn-rich towards the bath. Meanwhile, Fe and alloy elements, such as Ni and Cr, continue diffusing outward and dissipating into the bath. This growth process appears to be kinetically most favourable for the system.

Concurrent with the increased thickness of the reaction layer, selected areas within the reaction layer started to gather more Al and Fe and transformed into $Fe_2Al_5Zn_x$ particles as can be seen in Figs. 4b–d and 10. This transformation left other areas within the reaction layer depleted of Al to become even more Zn-rich, and could eventually transform into δ phases in some areas isolated from the bulk of the bath metal. Some of the transformed $Fe_2Al_5Zn_x$ particles were intimately connected with the top dross particles in the buildup, directly contributing to the growth of the buildup as shown in Fig. 5.

Conclusions

On-line testing of 316L SS was carried out in a galvanizing line. Examination of the tested samples revealed that 316L SS reacted with the galvanizing bath in the same way and to the same extent irrespective of the locations where they were placed. However, the attachment of suspended top dross particles to these samples (the buildup) varied significantly with the sample location. The corrosive reaction and formation of the $Fe_2Al_5Zn_x$ compound on sample surfaces served as the precursor for dross buildup on the samples. Important observations were made in the study:

1. The corrosive reaction of 316L SS with the galvanizing bath was initiated by the formation of an Al-rich layer consisting of the $Fe_2Al_5Zn_x$ compound which contained small amounts of Cr and Mo. The thickness of this reaction layer increased noticeably with the immersion time in the early stage, and then reached quasi-steady state when there was no noticeable change in thickness, indicating the reaction was controlled by a diffusion process.
2. Following the formation of the reaction layer, top dross particles suspended in the bath started to stick and build on this reaction layer because they possess the same crystallographic structure as the compound of the reaction layer. Some dross particles are intimately connected to the reaction layer while the majority of the particles are only loosely attached to the reaction layer.
3. The growth of the reaction layer was accomplished by a complicated phase evolution process within the layer. The Fe-aluminide reaction front continuously moved forward into the sample substrate, leaving behind a zone increasingly richer in Zn, which experienced a further phase transformation with the creation of $Fe_2Al_5Zn_x$ and Zn–Fe (δ) phase areas. Such an evolution in the phase constituents of the layer revealed clearly that Al supply necessary for the further growth of the $Fe_2Al_5Zn_x$ layer was largely unavailable following the formation of the buildup on the reaction layer. Al atoms diffusing toward the sample surface were largely consumed by the dross particles in the buildup. With an ample supply of Zn atoms, the phase evolution within the reaction layer observed in this study was the most kinetically favourable process under such a circumstance.
4. Fe dissolution from the incoming strip played a critical role in dross buildup on 316L SS. Samples placed in the immediate vicinity of the V region experienced significantly more buildup, revealing that the dross particle distribution in the galvanizing pot was not uniform and homogeneous.
5. Dross particles attached to samples welded to stationary supporting roll arms were generally smaller in size but numerous. In comparison, the particles built up on samples welded to the sides of the sink roll were much larger in size. This difference is believed to be the result of the differences in the melt-flow pattern and the Fe concentration gradient experienced by these two groups of samples. The turbulent flow created by the rotating sink roll and the ready availability of Fe dissolved from the incoming strip have a significant influence on the dross buildup process.
6. The larger mono-crystallite-like particles built on samples welded to the sides of the sink roll were the result of particle agglomeration.

Acknowledgements This project was financially supported by sponsors of the Galvanizing Autobody Program (GAP) managed by the International Lead Zinc Research Organization, Inc. The authors thank Teck Cominco Metals Ltd. and Nucor Steel for allowing

publication of this work. Mr. Artur B. Filc and Dr. Neil Gao provided assistance in sample preparation and examination. The manuscript was prepared with assistance from Mrs. Angeline M. Prskalo.

References

1. Horstmann D (1961) Proceedings of the 6th international conference on 'Hot Dip Galvanizing'. Interlaken, Switzerland, June 1961, pp 319–328
2. Nakagawa M, Sakai J, Ohkouchi T, Ohkoshi H (1996) Tetsu-to-Hagane 81(3):226–231
3. Brunnock MS, Jones RD, Jenkins GA, Llewellyn DT (1996) Ironmaking Steelmaking 23(2):171–176
4. Brunnock MS, Jones RD, Jenkins GA, Llewellyn DT (1996) Proc. Galvanizers Association. Chicago, IL, October 1996, pp 3–15
5. Nakagawa M, Sakai J, Ohkouchi T, Ohkoshi H (1995) Tetsu-to-Hagane 81(10):47–52 (English translation)
6. Gay B, Piccinin A, Dubois M (2001) Proc. Galvatech'01. Brussels, Belgium, June 2001, pp 262–269
7. Liu X, Barbero E, Irwin C, Sikka V, Hemrick J, Headrick W, Goodwin FE (2005) Proc. AISTech 2005. vol II, Charlotte, NC, May 9–12, 2005, pp 403–411
8. Zhang K (2005) ZCO-15-4 project report, ILZRO GAP Meetings. Charlotte, NC, May 2005
9. Dubois M (2005) Private communication, October 2005
10. Zhang K, Tang N-Y (2004) Mater Sci Technol 20:739–746
11. Ajersch F, Ilinca F, Hetu J-F, Goodwin FE (2005) Can Metall Quart 44(3):369–378
12. Metals Handbook (1990) vol 1, 10th edn, ASM International, Materials Park, OH, March 1990, pp 871–872
13. Tang N-Y, Adams GR (1993) The physical metallurgy of zinc coated steel. In: Marder AR (ed) The minerals, metals & materials society, pp 41–54